Plant Communications
Research Article

CellPress
Partner Journal

Multiple Alleles Encoding Atypical NLRs with Unique Central Tandem Repeats in Rice Confer Resistance to *Xanthomonas oryzae* pv. *oryzae*

Biaoming Zhang[1], Haitao Zhang[2,*], Fang Li[1], Yidan Ouyang[1], Meng Yuan[1], Xianghua Li[1], Jinghua Xiao[1] and Shiping Wang[1,*]

[1]National Key Laboratory of Crop Genetic Improvement, National Center of Plant Gene Research (Wuhan), Huazhong Agricultural University, Wuhan 430070, China

[2]State Key Laboratory of Biocatalysis and Enzyme Engineering, School of Life Sciences, Hubei University, Wuhan 430062, China

***Correspondence: Haitao Zhang (zht@hubu.edu.cn), Shiping Wang (swang@mail.hzau.edu.cn)**

https://doi.org/10.1016/j.xplc.2020.100088

ABSTRACT

Plants have developed various mechanisms for avoiding pathogen invasion, including *resistance* (*R*) genes. Most *R* genes encode nucleotide-binding domain and leucine-rich repeat containing proteins (NLRs). Here, we report the isolation of three new bacterial blight *R* genes in rice, *Xa1-2*, *Xa14*, and *Xa31*(*t*), which were allelic to *Xa1* and encoded atypical NLRs with unique central tandem repeats (CTRs). We also found that *Xa31*(*t*) was the same gene as *Xa1-2*. Although *Xa1-2* and *Xa14* conferred different resistance spectra, their performance could be attenuated by iTALEs, as has previously been reported for *Xa1*. XA1, XA1-2, XA14, and non-resistant RGAF differed mainly in the substructure of the leucine-rich repeat domain. They all contained unique CTRs and belonged to the CTR-NLRs, which existed only in Gramineae. We also found that interactions among these genes led to differing resistance performance. In conclusion, our results uncover a unique locus in rice consisting of at least three multiple alleles (*Xa1*, *Xa1-2*, and *Xa14*) that encode CTR-NLRs and confer resistance to *Xanthomonas oryzae* pv. *oryzae* (*Xoo*).

Keywords: multiple alleles, NLR, resistance, *Xanthomonas oryzae* pv. *oryzae*, iTALE, CTR

Zhang B., Zhang H., Li F., Ouyang Y., Yuan M., Li X., Xiao J., and Wang S. (2020). Multiple Alleles Encoding Atypical NLRs with Unique Central Tandem Repeats in Rice Confer Resistance to *Xanthomonas oryzae* pv. *oryzae*. Plant Comm. **1**, 100088.

INTRODUCTION

Plant diseases cause serious losses of biomass each year worldwide, leading to reduced crop yields and economic distress for farmers. Over time, plants have developed different survival mechanisms, such as *resistance* (*R*) genes. Most reported *R* genes encode nucleotide-binding domain and leucine-rich repeat containing proteins (NLRs) (Mermigka et al., 2020), which are typically classified into two groups based on the structure of their N-terminal sequences. The TNL (TIR-NLR) group contains a Toll/interleukin receptor (TIR) domain, whereas the CNL (CC-NLR) group contains a coiled-coil (CC) motif (van Wersch et al., 2020). The Arabidopsis genome has approximately 150 NLR-encoding genes, two-thirds of them encode TNLs and one-third encodes CNLs (Meyers et al., 2003). TNLs are absent from the genomes of many monocots (Jacob et al., 2013). In the rice genome, for instance, most of the 500+ NLR genes encode CNLs, and none encode TNLs (Meyers et al., 2005). However, recent studies have reported that many NLRs have additional integrated domains, such as the WRKY, kinase, and BED finger domains (Le Roux et al., 2015; Kroj et al., 2016; Bailey et al., 2018). *Yr7*, *Yr5*, and *YrSP* are recently cloned yellow rust resistance genes from hexaploid wheat (*Triticum aestivum*), all of which encode BED-domain-containing NLRs (BED-NLRs) (Marchal et al., 2018).

Many NLRs play important roles in rice defense, especially against fungi and insects. In interactions with *Magnaporthe oryzae*, 22 of the 26 isolated *R* genes encode NLRs (Fukuoka et al., 2014; Xu et al., 2014; Chen et al., 2015; Ma et al., 2015; Deng et al., 2017). Another nine NLR-encoding *R* genes have been isolated during rice–planthopper interactions (Du et al., 2009; Zhao et al., 2016). However, the interactions between rice and *Xanthomonas oryzae* pv. *oryzae* (*Xoo*), a pathogenic bacterium that causes bacterial blight, seem to be unique (Zhang and Wang, 2013). To date, 11 bacterial blight *R* genes have been isolated: *Xa1*, *Xa3*/*Xa26*, *Xa4*, *xa5*, *Xa10*, *xa13*, *Xa21*, *Xa23*, *xa25*, *Xa27*, and *xa41*(*t*) (Yoshimura

Published by the Plant Communications Shanghai Editorial Office in association with Cell Press, an imprint of Elsevier Inc., on behalf of CSPB and IPPE, CAS.

et al., 1998; Zhang and Wang, 2013; Tian et al., 2014; Hutin et al., 2015; Wang et al., 2015; Hu et al., 2017). These genes encode several different types of proteins that are involved in various aspects of rice-*Xoo* interactions (Zhang and Wang, 2013). Surprisingly, except for three receptor-like kinase-encoding bacterial blight *R* genes, the remaining eight genes are all related to transcription activator-like effectors (TALEs), which are secreted by *Xanthomonas* and *Ralstonia solanacearum* (Song et al., 1995; Sun et al., 2004; Zhang and Wang, 2013; Ji et al., 2016; Hu et al., 2017). TALEs can be translocated into plant cells via the type III secretion system (T3SS). Then, they directly bind to effector binding elements (EBEs), also called upregulated by TALE (UPT) boxes, in host genomic DNA by their central repeat region and promote gene expression (Boch et al., 2009; Romer et al., 2009; Antony et al., 2010). Three *Xoo* TALEs, AvrXa27, AvrXa10, and AvrXa23, bind to the EBEs of rice executor *R* genes *Xa27*, *Xa10*, and *Xa23* (Gu et al., 2005; Tian et al., 2014; Wang et al., 2015). Mutations in the EBEs of *xa13*, *xa25*, and *xa41*(*t*) retard interactions with *Xoo* TALEs PthXo1, PthXo2, AvrXa7, and Tal5 (Chu et al., 2006; Yang et al., 2006; Liu et al., 2011; Yuan et al., 2011; Hutin et al., 2015; Zhou et al., 2015). The recessive gene *xa5* encodes TFIIAγ5^{V39E} and attenuates the TALE-induced expression of rice genes (Gu et al., 2009; Yuan et al., 2016). The most interesting gene is *Xa1*, a BED-NLR, which recognizes multiple different TALEs and confers resistance (Yoshimura et al., 1998; Ji et al., 2016; Marchal et al., 2018). It has been reported that many full-length TALEs can trigger *Xa1*-mediated resistance. Meanwhile, interfering TAL effectors (iTALEs), in which Their N-terminals and transcription activation domains contain some deletions, can interfere with *Xa1*-mediated resistance. iTALEs exist in many *Xoo* and *Xoc* strains and may be responsible for the current narrow spectrum of *Xa1* (Ji et al., 2016).

Previously, *Xa2*, *Xa12*, *Xa14*, *Xa-25*, *Xa31*(*t*), and *Xa38* were reported to be localized to the region near *Xa1* and to confer race-specific resistance to *Xoo* (Ogawa et al., 1978; Gao et al., 2005; He et al., 2006; Cheema et al., 2008; Wang et al., 2009; Bao et al., 2010; Ellur et al., 2016). Furthermore, the uncloned *Xanthomonas oryzae* pv. *oryzicola* (*Xoc*) *R* gene, *Xo1*, which recognizes TALEs in an activation-domain-independent manner and can be suppressed by truncated TALEs, has also been mapped to the *Xa1* region (Read et al., 2016; Triplett et al., 2016). A recent report found two BED-NLR-encoding genes at the *Xo1* locus, including one that was highly similar to *Xa1* (Read et al., 2020). However, the relationships among these genes remain unclear.

Here, we report the isolation of three new allelic bacterial blight *R* genes, *Xa1-2*, *Xa14*, and *Xa31*(*t*), which are allelic to the previously isolated *Xa1*. Furthermore, we show that *Xa1*, *Xa1-2*, *Xa14*, and *Xa31*(*t*) all encode NLRs with unique central tandem repeats (CTRs), and that their homologs form a new class of NLR found only in Gramineae. We also demonstrate that interactions among *Xa1*, *Xa1-2*, and *Xa14* play complex roles in rice disease resistance to *Xoo*.

RESULTS

Xa14 Is Allelic to *Xa1*

Previously, the *Xa14* gene was mapped to a 300-kb region between markers HZR970-8 and HZR988-1 on chromosome 4 (Bao et al., 2010). To isolate *Xa14*, we inoculated an F_2 population of 599 individuals derived from a cross between rice cultivars IRBB14 and IR24, which carry and lack *Xa14*, respectively, with the *Xoo* strain PXO112, which triggers *Xa14*-mediated resistance in rice. After lesion length analysis, *Xa14* was further mapped between markers 52940 and RM5473 on chromosome 4 (Figure 1A). According to the reference sequence of the rice cultivar Nipponbare, there were 20 genes in this region, seven of which were predicted to encode NLRs (Figure 1B). Here, these genes were renamed *R-gene analogs RGAa* (Os04g52970), *RGAb* (Os04g53000), *RGAc* (Os04g53030), *RGAd* (Os04g53050), *RGAe* (Os04g53060), *RGAf* (Os04g53120), and *RGAg* (Os04g53160). *RGAb* and *RGAe* encoded proteins that contained only the leucine-rich repeat (LRR) domain. The other five genes encoded intact NLRs (Figure 1B). *RGAa*, *RGAc*, and *RGAd* encoded non-BED-NLRs, whereas *RGAf* and *RGAg* encoded BED-NLRs (Supplemental Figure 1A). Interestingly, both *RGAf* and *RGAg* were homologous to the isolated bacterial blight *R* gene *Xa1* (Supplemental Figure 1B). The genomic sequence of *RGAf* showed 84.7% identity to that of *Xa1*, whereas the sequence of *RGAg* showed only 59.8% identity (Supplemental Figure 1C). The homology of the 1-kb upstream sequences between *RGAf* and *Xa1* was 99.3%, but no significant homology was found in this region between *RGAg* and *Xa1*. These results suggest that *RGAf* was allelic to *Xa1* and that *RGAg* was a paralog of *Xa1*.

Further analysis showed that both *RGAg-BB14* and *RGAg-IR24*, the alleles of *RGAg* in IRBB14 and IR24, respectively, encoded truncated proteins. A single base insertion (A) at position 4068 was found in the genomic sequence of *RGAg-BB14*, leading to a frame shift and a subsequent stop codon. In *RGAg-IR24*, the truncation was caused by the deletion of 3945 "T" (Supplemental Figure 2A). *RGAf-IR24*, the allele of *RGAf* in IR24, also encoded a truncated protein due to a 5845 "C" deletion in the genomic sequence (Supplemental Figure 2B). Only *RGAf-BB14* encoded an intact NLR, and it showed 89.2% and 87.4% sequence identity to *Xa1* and *RGAf*, respectively (Supplemental Figure 2B). Thus, *RGAf-BB14* was the most likely *Xa14* candidate gene.

To test whether *RGAf-BB14* was *Xa14*, we transformed a native promoter-driven *RGAf-BB14* gene into the cultivar IR24. After transformation, 55 independent T_0 plants were generated and named RGAf-BB14-IR plants. These plants were inoculated with the *Xoo* strain PXO112 at the booting stage. All 26 positive plants showed significantly higher resistance compared with the negative plants and wild-type plants (Figure 1C, Supplemental Figure 3, and Supplemental Table 1). To further confirm the resistance, we inoculated three different T_1 lines derived from positive PXO112-resistance T_0 plants. Similarly, these positive T_1 plants were significantly more resistant than negative plantsand wild-type plants (Supplemental Figure 4). Similar results were obtained with transgenic Zhonghua11 (ZH11) and Mudanjiang8 (MDJ8) cultivars, both of which lack *Xa14* (Supplemental Figures 5 and 6; Supplemental Tables 2 and 3). These results strongly suggest that *RGAf-BB14* was *Xa14*.

In addition, bacterial growth ratios were analyzed using two positive and one negative RGAf-BB14-IR T_1 lines (Figure 1D).

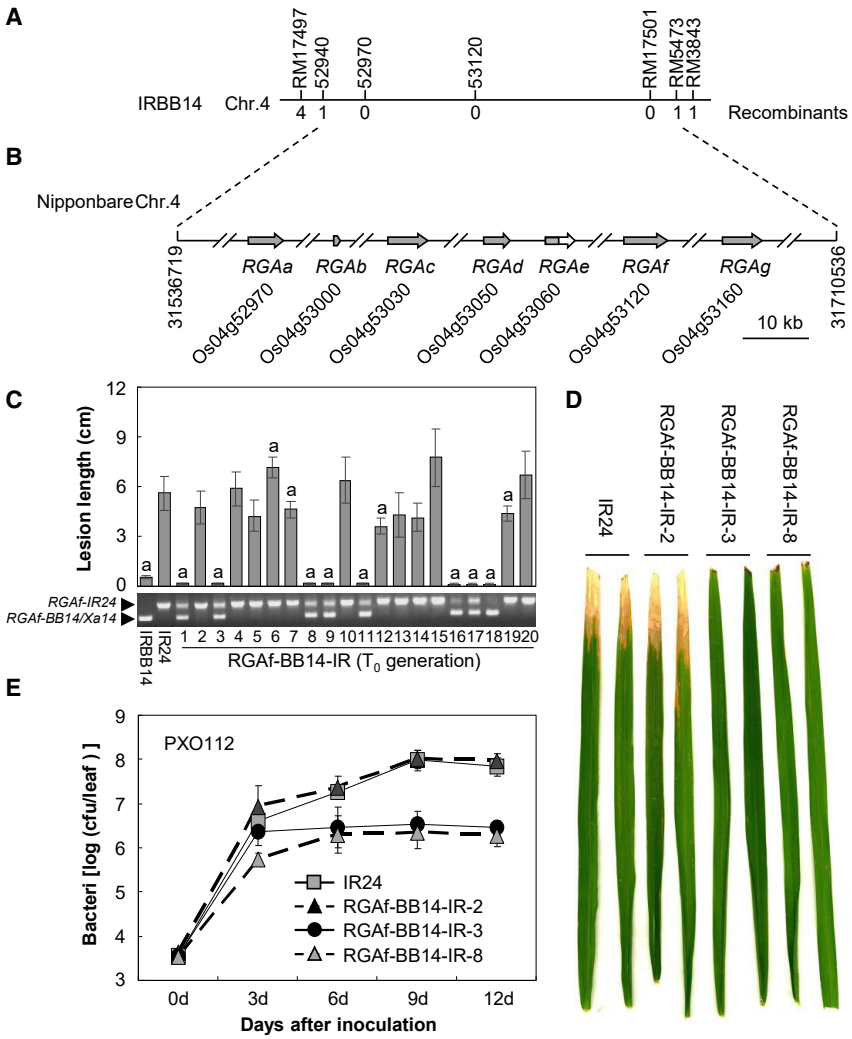

Figure 1. Mapping and Homology-Based Cloning of *Xa14*.

(A) Genetic map of the *Xa14* locus.

(B) Physical map and candidate genes of the *Xa14* locus in the corresponding region of Nipponbare. Arrows indicate *RGA* genes. The gray arrow/box indicates the coding region. The white arrow indicates the non-coding region.

(C) Lesion length analysis of RGAf-BB14-IR T_0 plants after inoculation with the *Xoo* strain PXO112. Significant differences were detected between IR24 and transgenic plants or IRBB14 at $P < 0.01$ (indicated with "a").

(D) Leaves of RGAf-BB14-IR lines inoculated with the *Xoo* strain PXO112.

(E) Bacterial growth ratio in RGAf-BB14-IR lines after inoculation with the *Xoo* strain PXO112. cfu, colony-forming units.

Data are presented as mean ± SD.

Bacterial growth in RGAf-BB14-IR-3 and RGAf-BB14-IR-8 was only 2.4%–21.2% of the wild-type plants at 6–12 days after infection, whereas bacterial growth in RGAf-BB14-IR-2 was 103.2%–138.9% of the wild type (Figure 1E). These results indicate that the resistance mediated by *Xa14* was associated with reduced bacterial growth in plants.

Xa1-2 and *Xa31(t)* Are Also Allelic to *Xa14* and *Xa1*

It has been reported that *Xa2* and *Xa31(t)* are also localized to a region near *Xa1* or *Xa14* and that both confer race-specific resistance to *Xoo* (He et al., 2006; Wang et al., 2009). Therefore, *Xa14* and *Xa1* alleles in donors IRBB2 and Zhachanglong (ZCL) (referred to as *RGAf-BB2* and *RGAf-ZCL*, respectively, hereafter) were likely *Xa2* and *Xa31(t)* candidate genes. Surprisingly, the genomic sequences of *RGAf-BB2* and *RGAf-ZCL* were completely identical. Only five polymorphisms, nucleotide deletions or substitutions, were identified more than 500 bp upstream of the predicted transcription start site in each gene (Figure 2A). Compared with the *RGAf* genes from cultivars MDJ8 and ZH11, designated *RGAf-MDJ8* and *RGAf-ZH11*, respectively, the genomic sequence of *RGAf-BB2* (or *RGAf-ZCL*) was more similar to those from *Xa1* and *Xa14* (Supplemental Figure 7A). The main difference between *RGAf-BB2* and *Xa1* was a 279-bp deletion in the LRR-encoding region, the remaining sequence of *RGAf-BB2* showed 99.9% identity to that of *Xa1* (Supplemental Figure 7B). Compared with *Xa14*, a low-homologous region existed in *RGAf-BB2* but the two remaining regions showed 99.0% and 89.8% identity to the corresponding regions in *Xa14* (Supplemental Figure 7B). These results indicate that *RGAf-BB2* and *RGAf-ZCL* may confer *Xoo* resistance.

To investigate this possibility, we transformed a native promoter-driven *RGAf-BB2* gene into cultivars ZH11 and MDJ8. The transgenic plants were named RGAf-BB2-ZH and RGAf-BB2-MDJ, respectively. *Xa2 has* previously been reported to confer resistance to the *Xoo* strain T7147, consistently, the IRBB2 plants obtained in this study showed resistance to T7174 (He et al., 2006). Additionally, in 30 RGAf-BB2-ZH T_0 plants, 21 positive plants were highly resistant to T7174 compared with negative plants and wild-type plants (Figure 2B). The resistance was confirmed in three RGAf-BB2-ZH T_1 lines (Supplemental Figure 8) and similar results were obtained with RGAf-BB2-MDJ plants (Supplemental Figure 9A and 9B). Furthermore, bacterial growth and lesion length were significantly reduced at 6–12 days in two positive T_1 lines (Figure 2C and 2D). Although these results strongly suggest that *RGAf-BB2* was the *Xa2* gene, we named it *Xa1-2* to avoid confusion.

Xa31(t) has previously been reported to mediate resistance to the Chinese *Xoo* strain OS105. Considering the sequence identity between *RGAf-BB2* and *RGAf-ZCL*, IRBB2 plants were inoculated with OS105 to determine whether *Xa1-2* could confer resistance. Indeed, IRBB2 plants were highly resistant to OS105 (Supplemental Figure 10A), and resistance was also present in RGAf-BB2-ZH-3 and RGAf-BB2-ZH-6 plants (Supplemental Figure 10B). These results strongly indicate that *Xa31(t)* and *Xa1-2* were the same gene.

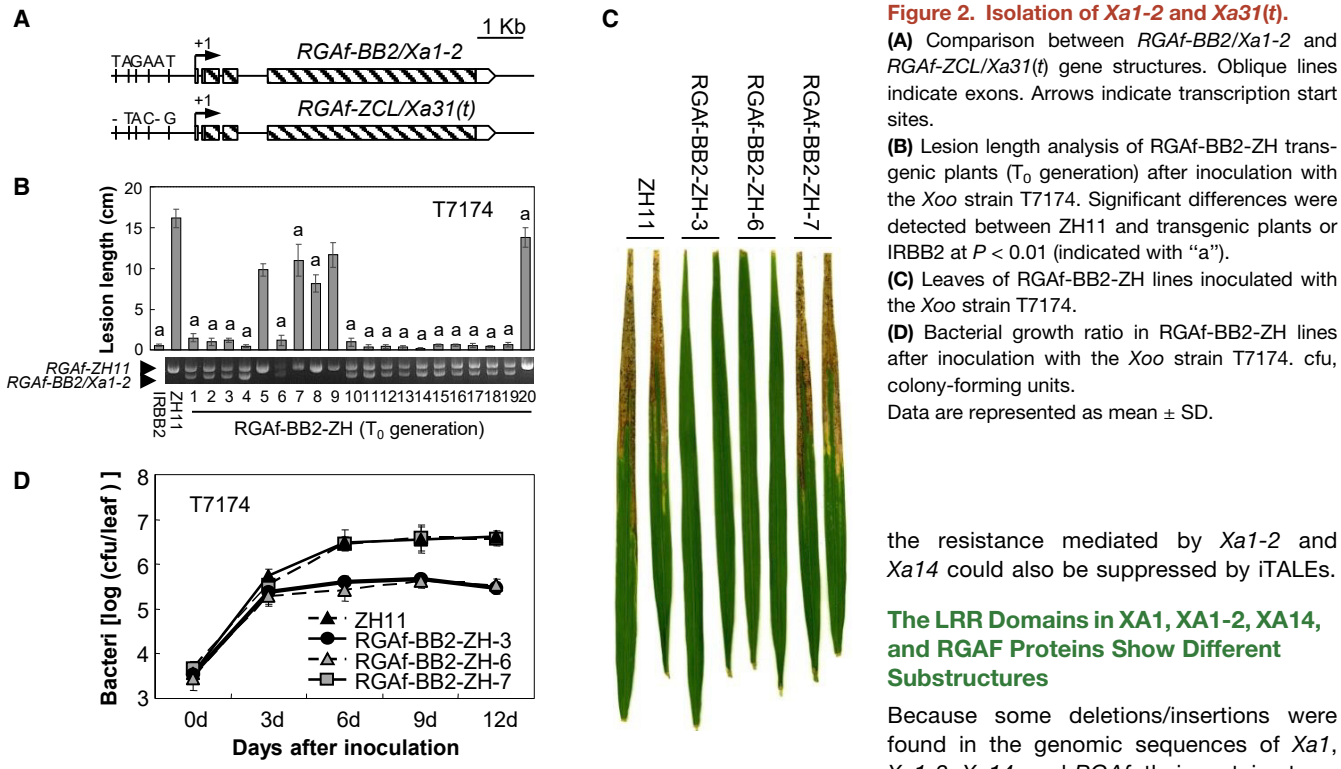

Figure 2. Isolation of *Xa1-2* and *Xa31(t)*.

(A) Comparison between *RGAf-BB2/Xa1-2* and *RGAf-ZCL/Xa31(t)* gene structures. Oblique lines indicate exons. Arrows indicate transcription start sites.

(B) Lesion length analysis of RGAf-BB2-ZH transgenic plants (T_0 generation) after inoculation with the *Xoo* strain T7174. Significant differences were detected between ZH11 and transgenic plants or IRBB2 at $P < 0.01$ (indicated with "a").

(C) Leaves of RGAf-BB2-ZH lines inoculated with the *Xoo* strain T7174.

(D) Bacterial growth ratio in RGAf-BB2-ZH lines after inoculation with the *Xoo* strain T7174. cfu, colony-forming units.

Data are represented as mean ± SD.

In addition, IRBB1 and IRBB14 plants were also resistant to OS105 (Supplemental Figure 10A). Transgenic plants carrying *Xa1* in a ZH11 background (referred to as Xa1-ZH plants hereafter) and RGAf-BB14-ZH plants also showed OS105 resistance (Supplemental Figure 10B). Moreover, all of the Xa1-ZH, RGAf-BB2-ZH, and RGAf-BB14-ZH plants showed resistance to the *Xoo* strain T7174 (Supplemental Figures 10B, 11, and 12). RGAf-BB14-ZH and Xa1-ZH plants were resistant to T7133 whereas RGAf-BB2-ZH plants were as susceptible as ZH11 (Supplemental Figure 10B), and neither *Xa1* nor *Xa1-2* conferred resistance to PXO112 and PXO280 (Supplemental Figure 10A and 10B). These results indicate that *Xa1*, *Xa1-2*, and *Xa14* each had a unique resistance spectrum.

iTALEs Suppress *Xa1-2*- and *Xa14*-Mediated Resistance

Xa1 has previously been reported to confer *Xoo* resistance by recognizing multiple full-length TALEs, and this resistance can be attenuated by some iTALEs, such as Tal3a and Tal3b in PXO99 (Ji et al., 2016). To determine whether *Xa1-2* and *Xa14* function in a similar way, we inoculated plants carrying these genes with PXO99 and PB, a mutant in which both *Tal3a* and *Tal3b* are knocked out (Ji et al., 2016). After inoculation with PXO99, IRBB2 and IRBB14 plants were as susceptible as IRBB1 and IR24 plants. By contrast, PB-inoculated IRBB2 and IRBB14 plants showed significant resistance, similar to that observed for the IRBB1 plants (Figure 3A). Moreover, similar results were obtained with transgenic plants that carried *Xa1-2* and *Xa14*. In contrast to the PXO99 inoculation, the PB inoculation rendered RGAf-BB2-ZH and RGAf-BB14-ZH plants more resistant, similar to that observed for Xa1-ZH plants (Figure 3B and Supplemental Figure 13). These results strongly suggest that the resistance mediated by *Xa1-2* and *Xa14* could also be suppressed by iTALEs.

The LRR Domains in XA1, XA1-2, XA14, and RGAF Proteins Show Different Substructures

Because some deletions/insertions were found in the genomic sequences of *Xa1*, *Xa1-2*, *Xa14*, and *RGAf*, their protein structures were analyzed to identify motifs that were essential for resistance. The N-terminal sequences of the four proteins were highly conserved, and all consisted of a BED finger domain and a nucleotide-binding (NB) domain (Figure 4A). Interestingly, the LRR domains of the four proteins all contained nearly perfect tandem repeats, named CTRs here. Each CTR in the four proteins was composed of 93 highly conserved amino acids (Figure 4B) but the repeat numbers varied from four to six (Figure 4A). XA1 was found to have six repeats, R1 to R6. Compared with XA1, a deletion of a whole repeat was found in XA1-2 (Figure 4A; Supplemental Figures 14 and 15), and XA14 and RGAF both contained only four repeats (Figure 4A). In addition to the repeats, all proteins contained homologous regions in the N and C termini of the LRR domains, designated here the Initial and Terminal LRR, respectively (Figure 4A). XA14 contained an additional motif between the Initial LRR and CTRs, designated the Linker, that was not present in XA1 and XA1-2 (Figure 4A and Supplemental Figure 16). RGAF contained an identical Linker compared with XA14 but a unique motif not found in the other three *R* proteins; this motif was designated the intervening motif (Figure 4A and Supplemental Figure 17). Further analysis showed that the intervening motif was also present in RGAF-IR24, RGAF-MDJ8, and RGAF-ZH11, which were encoded by other non-resistant alleles (Supplemental Figure 18). Very recently, a study described the CTRs of XA1, RGAF, and CGS-Xo1$_{11}$ (Read et al., 2020). In this work, the CTRs were described as beginning at a different amino acid residue. According to our results, they belonged to the Initial LRR and were separated by the Linker or intervening motif in XA14 and RGAF. Our CTR classification was based on substructural comparisons among the four proteins and is thus more conducive to application.

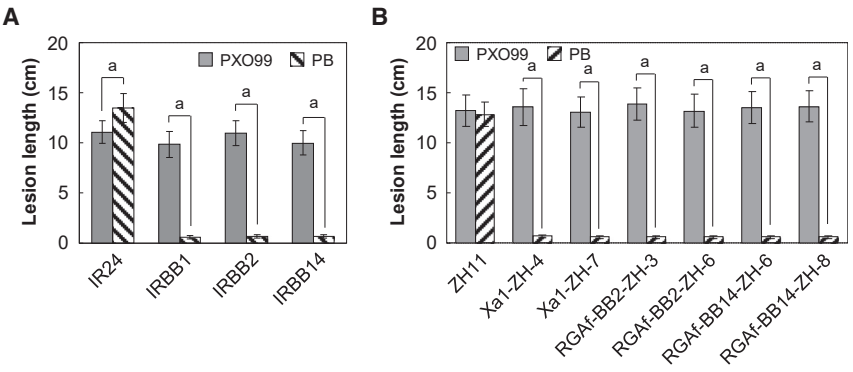

Figure 3. *Xa1-2*- and *Xa14*-Mediated Resistance Can Be Attenuated by iTALEs.

(A) Lesion length analysis of IR24, IRBB1, IRBB2, and IRBB14 plants after inoculation.

(B) Lesion length analysis of ZH11 and transgenic lines carrying *Xa1*, *Xa1-2*, and *Xa14* after inoculation. All the plants were inoculated with *Xoo* strains PXO99 and PB, a mutant in which both iTALEs are knocked out. The letter "a" indicates a significant difference between the two treatments at $P < 0.01$.

To understand the geographic distributions and relationships among different alleles, we analyzed the frequency of each allele in a collection of 520 rice cultivars using PCR markers. Most accessions were of the *RGAf* type, followed by the *Xa14* type, which was especially common in *indica* rice. Both the *Xa1* and *Xa1-2* types were rare (Figure 4C and Supplemental Table 4) but their frequencies varied among different geographic areas. Interestingly, approximately one-fifth of the accessions from China were of the *Xa14* type. In addition, several accessions from the Indian subcontinent and South Pacific area were of the *Xa14* type (Figure 4D, Supplemental Figure 19, and Supplemental Table 4). The *Xa1* type had a relatively higher frequency in the United States and the Indian subcontinent than other areas, and the *Xa1-2* type was more frequently found in the United States and Southeast Asia. Also, in some areas such as Africa and Western Europe, all accessions were of the *RGAf* type (Figure 4D, Supplemental Figure 19, and Supplemental Table 4). These results suggest that these alleles were selected differentially in different regions, a phenomenon that may be partly related to the different geographic distributions of various *Xoo* strains.

XA1, XA1-2, XA14, and RGAF Belong to a Unique NLR Class Specific to Gramineae

To understand the evolutionary history of XA1, XA1-2, XA14, and RGAF, we searched for homologous proteins using protein BLAST at NCBI and the MSU Rice Genome Annotation Project (RGAP) Database, as well as sequences obtained from relevant articles. In Nipponbare, only RGAG, RGAD, and LOC_Os04g22090.1 were classified as homologs. Other *RGA* proteins at the *Xa1* locus failed to show high enough homology to RGAF (Supplemental Figure 20). Orthologs of the *RGA* proteins in IR24, IRBB1, and IRBB14 were not included, as they were highly conserved relative to corresponding proteins in Nipponbare and were not representative, with the exception of XA1, XA1-2, and XA14. We ultimately obtained 100 homologs, including RGAF. Surprisingly, all homologs were from Gramineae (Supplemental Table 5).

The homologs could be classified into five groups based on full-length protein-based phylogeny and substructure analysis (Figure 5A and 5B; Supplemental Table 6). Three-fourths of them belonged to group I, which contained all motifs, including Initial LRR, intervening motif, Linker, CTRs and Terminal LRR, in their LLR regions, such as RGAF (Figure 5A–5C). NLRs encoded by yellow rust resistance genes *Yr5* and *Yr7* in *Triticum aestivum* also belonged to group I (Figure 5B). Group II was composed of eight homologs without the Linker in their LRR domains. Among the eight group II homologs, six came from *Triticum turgidum*, *Triticum urartu*, and *Aegilops tauschii*, which are genome donors of common wheat, one from *Oryza glumaepatula*, a kind of wild rice, and one from *Leersia perrieri*, the nearest outgroup of genus *Oryza* (Figure 5B and 5C). XA14, which did not contain the intervening motif, was the only protein in group III (Figure 5A and 5B). XA1 and XA1-2 belonged to group IV, whose members contained neither the Linker nor the intervening motif in the LRR region (Figure 5A). One homolog from *L. perrieri* was also included in this group (Figure 5B). Group V was composed of different types of truncated proteins from various species (Figure 5A–5C). Notably, almost all members of groups II, III, and IV appeared later than group I members in the same clade, suggesting that they may have arisen from group I homologs as a result of motif deletions (Figure 5B).

Notably, the BED finger domain in RGAF, XA1, XA1-2, and XA14 was missing from approximately one-third of the RGAF homologs. Thus, groups I, II, and V could be further divided into two subgroups, a and b, based on the presence or absence of the BED finger domain (Figure 5A and 5B; Supplemental Table 6). Except for members from group V, all other homologs contained the Initial LRR, Terminal LRR, and CTRs, which varied in number from one to nine units, and showed high levels of sequence conservation in CTRs (Supplemental Table 7). These results suggest that the substructure of LRR is essential and conserved during evolution. Thus, all CTR-containing homologs could be classified as CTR-NLRs. Together, these results clearly demonstrate that CTR-NLRs constitute a unique class of NLRs in Gramineae.

Interactions among *Xa1*, *Xa1-2*, and *Xa14* Lead to Differences in Rice Disease Resistance

Dimerization or oligomerization through the TIR or CC domain has been observed in some NLRs (Bernoux et al., 2011; Maekawa et al., 2011; Deng et al., 2017; Wang et al., 2019), however, whether BED-NLRs, such as XA1, XA1-2, and XA14, interact with themselves or with one another remain elusive. In yeast, the BED finger domain of XA1 and XA14, designated XA1-BED and XA14-BED, respectively, could interact with themselves or with one another (Figure 6A and Supplemental Figure 21A). However, these interactions were weak and could be disrupted by the NB domain (Supplemental Figure 21B–21D). Similar interactions were found in rice protoplasts, and all interactions appeared to occur in the nuclei (Figure 6B). To further confirm

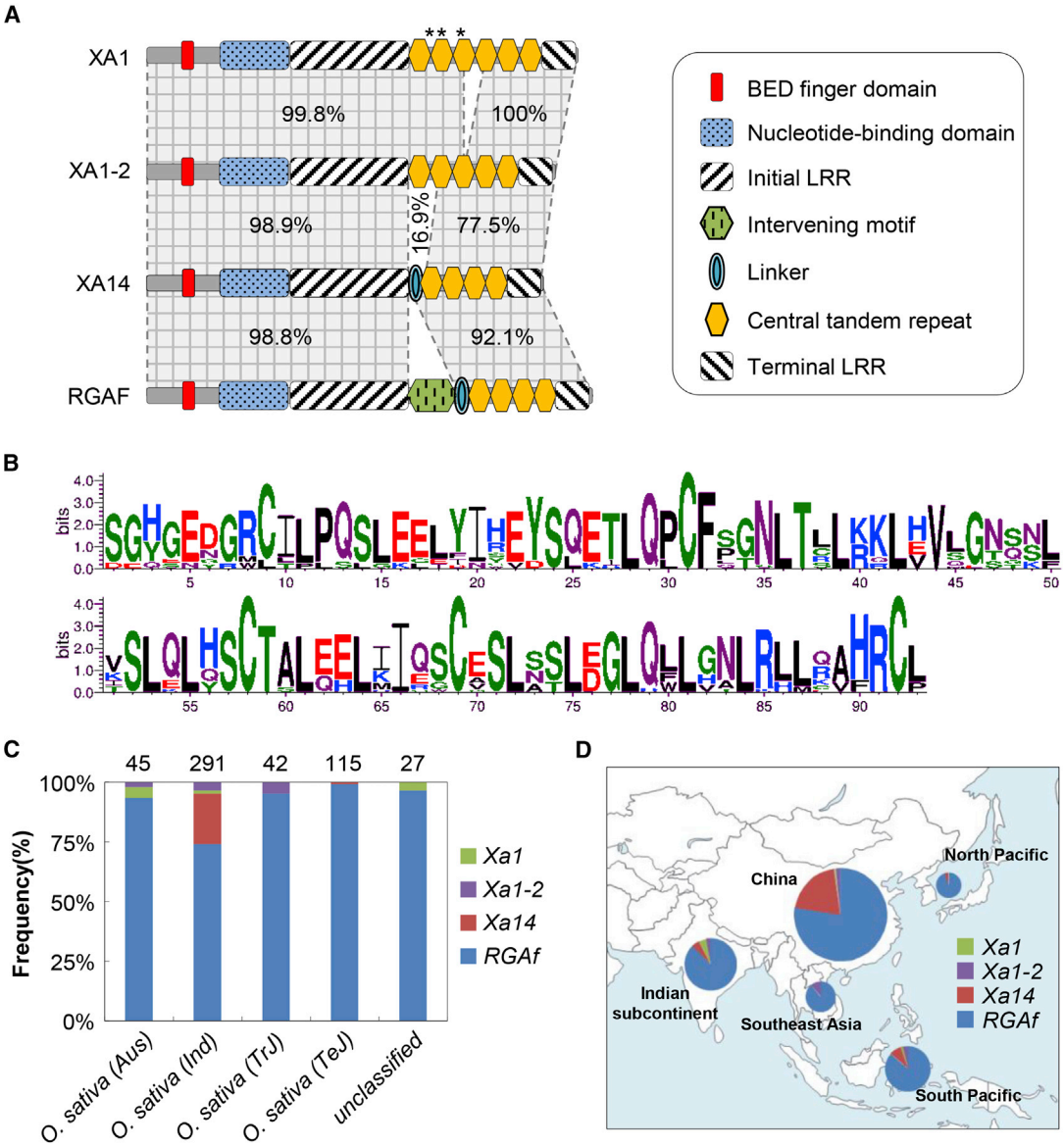

Figure 4. Different Substructures and Distributions of XA1, XA1-2, XA14, and RGAF.

(A) Domains and motifs in XA1, XA1-2, XA14, and RGAF. Percentages indicate sequence identity. Stars indicate missense mutations.

(B) Conserved amino acid residues in the CTRs of the four proteins shown by WebLogos.

(C) Ratios of *Xa1*, *Xa1-2*, *Xa14*, and *RGAf* alleles in the rice variety collection. Numbers above the columns indicate the total accession numbers of the corresponding subpopulation.

(D) Geographic distribution of *Xa1*, *Xa1-2*, *Xa14*, and *RGAf* haplotypes in tropical and temperate regions in Asia. Relative frequencies of the haplotypes in each area are represented by the colored sectors of the pie chart. The size of the pie chart is proportional to the number of varieties.

these results, we expressed XA1-BED and XA14-BED labeled with 3×FLAG or 9×Myc in tobacco leaves for co-immunoprecipitation. The results show that XA1-BED and XA14-BED could form both homo- and heterocomplexes (Figure 6C). Given that the BED finger domain in XA1-2 (XA1-2-BED) is identical to that in XA1-BED, similar interactions may exist among XA1-BED, XA1-2-BED, and XA14-BED.

Further analysis using hybrids derived from IRBB1, IRBB2, and IRBB14 showed that these interactions could impede rice disease resistance. The IRBB14/IRBB1 hybrid was more susceptible to the *Xoo strain PXO112* compared with the IRBB14 parent (Figure 7A). Similar results were obtained with the reciprocal hybrid IRBB1/IRBB14 (Figure 7B) and the F_2 plants derived from both the IRBB14/IRBB1 and IRBB1/IRBB14 crosses (Supplemental Figure 22). Next, the IRBB1/IRBB14 F_2 individuals were inoculated with T7174, to which both IRBB1 and IRBB14 plants were resistant. Surprisingly, the hybrid showed greater susceptibility than either IRBB1 or IRBB14 plants (Figure 7C). Similar results were obtained with T7174-inoculated IRBB2/IRBB14 F_2 plants (Supplemental Figure 23). By contrast, the IRBB1/IRBB2 hybrid exhibited the same level of resistance as IRBB1 and IRBB2 when inoculated with T7174 (Figure 7D). These results suggest that interactions

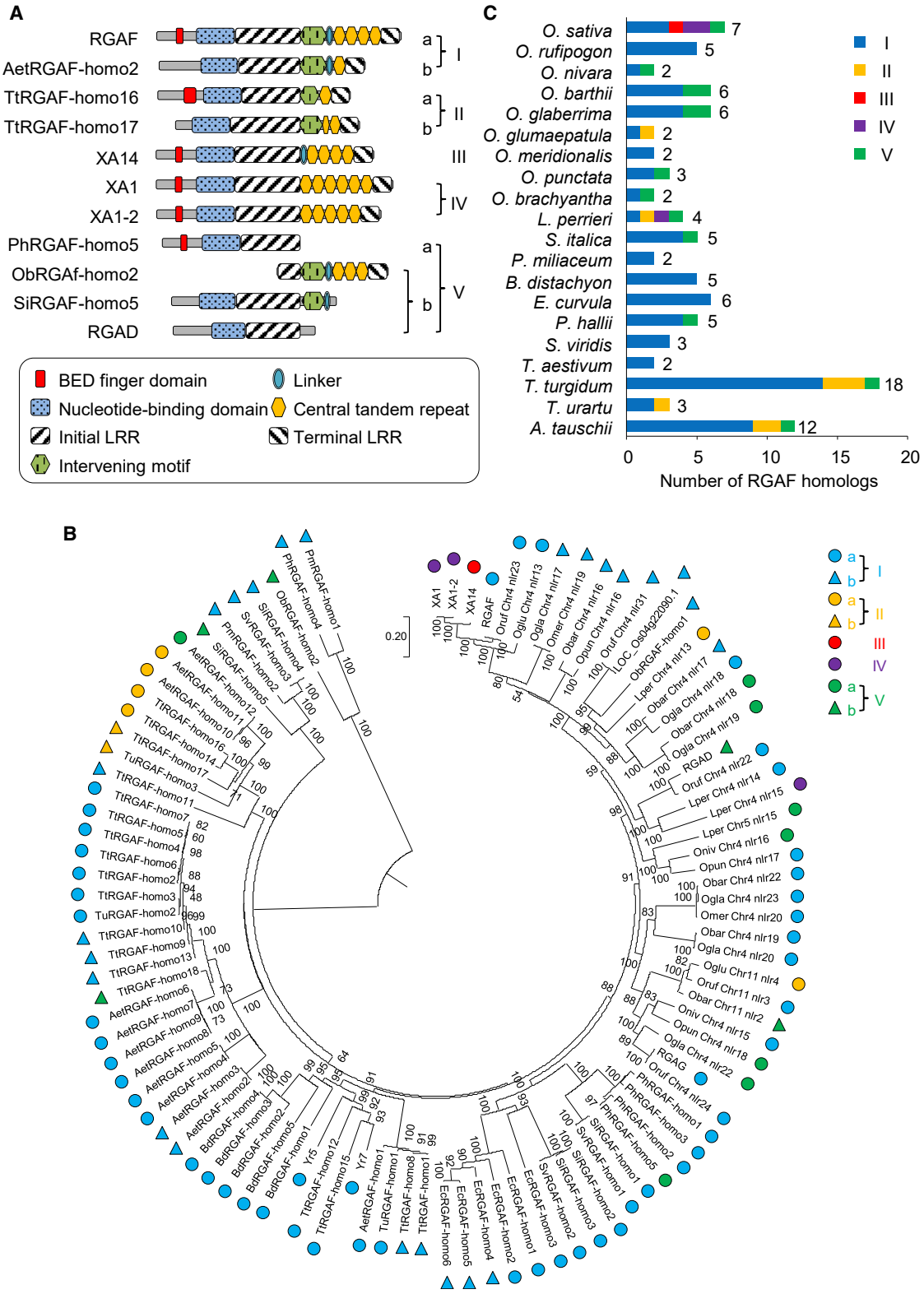

Figure 5. RGAF Homologs Existed only in Gramineae.

RGAF homologs could be clustered into five groups, denoted I–V. Subgroups are indicated by a and b.

(A) Classification of RGAF homologs.

(B) Full-length protein-based phylogeny of RGAF homologs identified by BLAST as described in Methods. Numbers on the interior branches indicate the bootstrap support values (%; only values greater than 50% are shown) from 1000 replicates.

(C) Number of RGAF-homolog in each group in different Gramineae species. Numbers on the right of the columns indicate numbers of RGAF homologs.

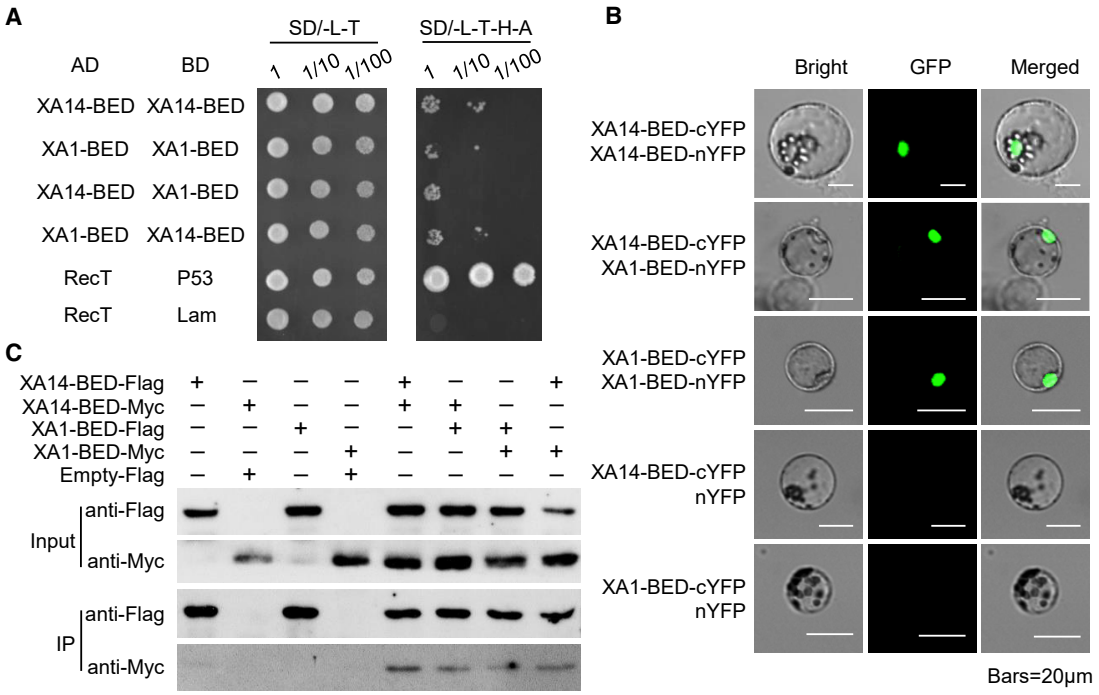

Figure 6. XA14-BED and XA1-BED Interact with Themselves and One Another.

(A) XA14-BED and XA1-BED interact with themselves and one another in yeast. RecT and P53 were used as positive controls, and RecT and Lam were used as negative controls.

(B) XA14-BED and XA1-BED interact with themselves and one another in rice protoplasts. cYFP, C-terminal portion of YFP; nYFP, N-terminal portion of YFP.

(C) Interactions between XA1-BED and XA14-BED are confirmed in a co-immunoprecipitation assay. IP, immunoprecipitation.

between XA14 and XA1 or XA1-2 impaired resistance, whereas the interaction between XA1 and XA1-2 did not.

DISCUSSION

Allelic variation is very important for the evolution of functional genes in plants. Several formerly identified genes were subsequently found to be alleles of the same gene, this phenomenon is especially common among resistance genes. In rice, many blast resistance genes are allelic. For example, *Pik*, *Pikm*, *Pik-p*, *Pi1*, and *Pike* are allelic to one another, *Pi2* is allelic to *Piz-t*, and *Pid3* is allelic to *Pi25* (Zhang and Wang, 2016). There are also multiple alleles of *Brown planthopper* (*BPH*) *R* genes. After *BPH9* was cloned, another eight *BPH* genes were found to be allelic to it (Zhao et al., 2016). Here, we showed that in rice–*Xoo* interactions, *Xa1*, *Xa1-2*, and *Xa14* are allelic, and *Xa31*(*t*) is the same as *Xa1-2*. There are still other uncloned *R* genes located near this locus, such as *Xa12*, *Xa-25*, *Xa38*, and *Xo1* (Ogawa et al., 1978; Gao et al., 2005; Cheema et al., 2008; Ellur et al., 2016; Triplett et al., 2016). Although it is difficult to confirm that these are also alleles due to the lack of related germplasms, our results show that variations in this gene play important roles in *Xoo* resistance in rice.

Interestingly, similar to *Xa1, Xa1-2*- and *Xa14*-mediated resistance can be attenuated by iTALEs, and it is likely that endogenous iTALEs in some *Xoo* strains make them compatible with plants that carry *Xa1*, *Xa1-2*, or *Xa14*. However, whether there are direct physical interactions between iTALEs (or TALEs) and XA1 or XA1-like NLRs remains unclear, and our ongoing experiments suggest that iTALEs may only partially contribute to the different resistance spectra of *Xa1*, *Xa1-2*, and *Xa14* (data not shown). This is consistent with a previous report that some iTALEs also exist in many IRBB1-incompatible *Xoo* strains and fail to suppress *Xa1*-mediated resistance (Ji et al., 2016). TALE-encoding genes contain a large portion of repetitive sequence and are multi-copied in many *Xoo* strains, therefore, the full characterization of all TALE-encoding genes in different *Xoo* genomes will facilitate future studies.

The different LRR domain substructures of XA1, XA1-2, XA14, and RGAF homologs may be the main reason for the differences in *Xoo* resistance. Sequences that encode the intervening motif were present in many non-resistant alleles, such as *RGAf*, *RGAf-IR24*, *RGAf-MDJ8*, and *RGAf-ZH11*. It seems that the intervening motif may affect the function of other motifs and lead to susceptibility. The Linker, however, may associate with other motifs during the *Xoo*–rice interaction, as *Xa14* exhibited a different resistance spectrum compared with *Xa1* and *Xa1-2*. It is likely that the Linker makes the conformation of XA14 slightly different from those of XA1 and XA1-2 and leads to changes in the recognition of potential interacting proteins, perhaps including some TALEs. However, the Linker and intervening motifs were reported here for the first time, and further studies are required to fully characterize their functions in resistance.

It is also interesting that XA1, XA1-2, XA14, RGAF, and their homologs all contain CTRs in the LRR region. The CTRs were well

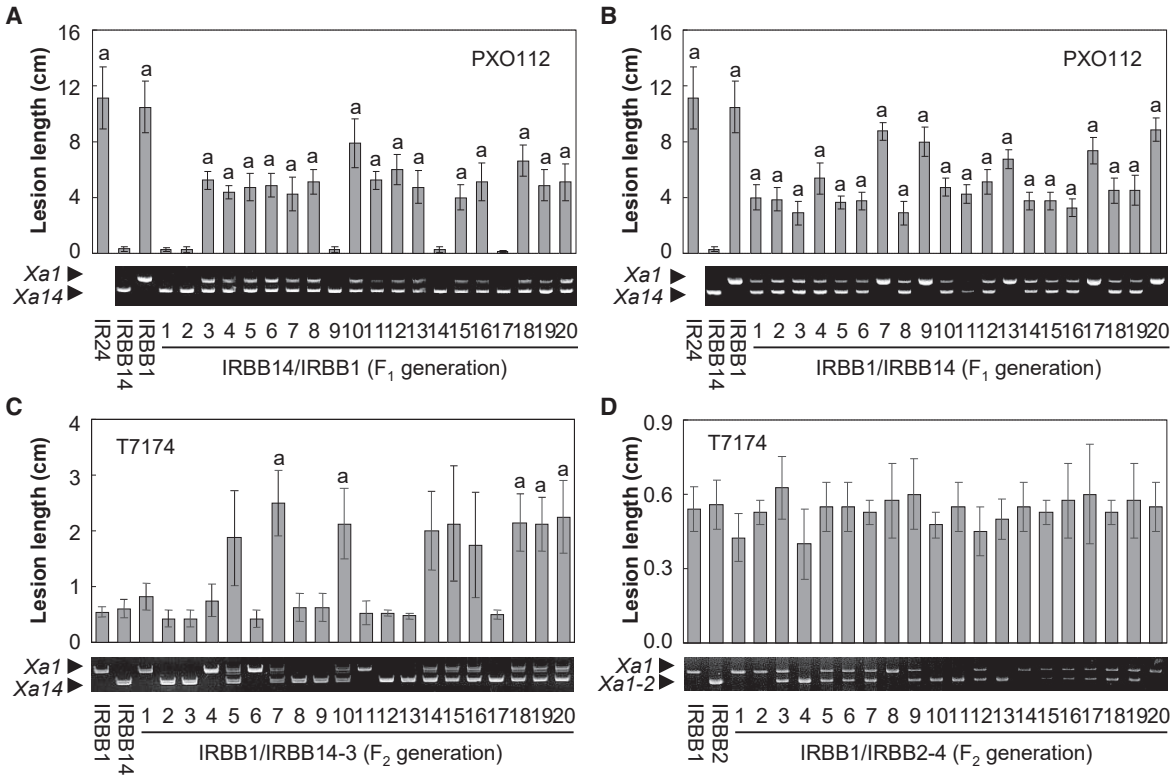

Figure 7. Interactions among *Xa1*, *Xa1-2*, and *Xa14* Lead to Differences in Rice Resistance.

(A) Lesion length analysis in IRBB14/IRBB1 F_1 hybrids after PXO112 inoculation.

(B) Lesion length analysis in IRBB1/IRBB14 F_1 hybrids after PXO112 inoculation.

(C) Lesion length analysis in IRBB1/IRBB14-3 F_2 plants after T7174 inoculation.

(D) Lesion length analysis in IRBB1/IRBB2-4 $F_{2\ plants}$ after T7174 inoculation.

Data are presented as mean ± SD. The letter "a" indicates a significant difference compared with IRBB14 at $P < 0.01$.

conserved in sequence but varied in numbers even within the same species. This may be the result of adaptation and evolution, generating new genes to cope with different pathogens. The molecules or sequences with which CTRs can interact remain completely unknown and present an interesting question for future investigation.

The Phylogenetic analysis of RGAF homologs demonstrated that XA1, XA1-2, XA14, and RGAF clustered in the same clade and appeared later than many other homologs (Figure 5B). Thus, it is likely that *RGAf* first originated from an ancestral gene in a wild rice variety and *Xa14* then originated from *RGAf*, as suggested by the deletion of the intervening motif-encoding sequence. *Xa1* and *Xa1-2* may have arisen from *Xa14*, as suggested by the deletion of the Linker-encoding sequence. However, it is difficult to determine whether *Xa1* or *Xa1-2* is the ancestral gene, as the gain and loss of a CTR-encoding sequence may occur at a similar frequency. Moreover, the possibility that other paralogs were involved in the evolution of these genes cannot be excluded. A recent report showed that the *Xo1* locus has expanded and contains 14 predicted NLRs in the rice cultivar Carolina Gold Select (Read et al., 2020). Further investigation of the exact number and content of NLR-encoding genes at this locus in IRBB1, IRBB2, IRBB14, and other rice cultivars will contribute to our understanding of the evolution of these genes.

Xa1, *Xa1-2*, and *Xa14* encode atypical NLRs that contain the BED finger domain, and we found that the BED finger domains of XA1, XA1-2, and XA14 could interact with themselves or with one another. Although there were other possibilities, such as their full-length proteins being unable to interact with one another or interactions with other RGAs or BED-containing proteins, the varied resistance of the progenies of crosses among IRBB1, IRBB2, and IRBB14 nonetheless provided insight into the complex relationships among *Xa1*, *Xa1-2*, and *Xa14*. One-fifth of rice cultivars in China carry the *Xa14* gene whereas cultivars from other areas are more likely to contain *Xa1* or *Xa1-2*. The results presented here may be helpful for further applications of NLRs, such as *Xa1*, *Xa1-2*, and *Xa14*, especially in hybrid rice breeding and production.

In addition, BED fingers were previously found to be DNA-binding domains in many transposases and chromatin-boundary-element-binding proteins (Aravind, 2000). Although it has been described as an integrated decoy domain, evidence is still needed for the cloned BED-NLRs. The BED domains in XA1, XA1-2, XA14, and even RGAF were highly conserved and were thus less likely to be decoys than LRR domains. Also, it seems unreasonable that these BED-NLRs contained two decoy domains separated by an NB domain, as most confirmed decoys are located at the C terminus of NLRs (Cesari et al., 2013; Le Roux et al., 2015). Although the mechanisms by which the BED

domain functions in the defense process are largely unknown, the atypical architecture of BED-NLRs strongly suggests that they will provide new insights into plant immunity.

METHODS

Plasmid Construction and Rice Transformation

Each of the fragments containing native promoter-driven *Xa14*, *Xa1*, or *Xa1-2* was obtained using restriction endonuclease digestion and ligation from three PCR products using IRBB14, IRBB1, and IRBB2 genomic DNA, respectively, as templates. PCRs were performed using the Xa2-7F-2/Xa14-19R, Xa2-12F-2/Xa2-14R, and Xa2-8F-K/Xa14-8R primers (Supplemental Table 8). The PCR products were digested by *Bam*HI/*Hin*dIII, *Bam*HI/*Sac*I, and *Bam*HI/*Kpn*I, respectively, and ligated one after another into a modified pC1301 vector, in which the *Sac*I site had been deleted.

All constructs were delivered separately into the *Agrobacterium tumefaciens* strain EHA105. Rice transformation was then performed using the calli of rice variety IR24, Zhonghua 11, or Mudanjiang 8 by the *Agrobacterium*-mediated method (Lin and Zhang, 2005).

Pathogen Inoculation

The *Xanthomonas oryzae* pv. *oryzae* strains used in this study included Japanese races T7174, T7147, and T7133, Chinese strains OS105 and FuJ23, Philippine strains PXO99, PXO112, and PXO280, and PB, which is an engineered mutant generated from PXO99 (Ji et al., 2016). All strains were cultured on potato-based medium for 2 days at 28°C. Rice plants were inoculated with *Xoo* strains at the booting (panicle development) stage by the leaf-clipping method (Chen et al., 2002). Lesion lengths were measured 14 days after inoculation. All inoculations were repeated at least twice with similar results, and only one replicate per inoculation is presented.

WebLogos

WebLogos showing the conserved amino acid residues of the CTRs were generated with WebLogo 3 (https://weblogo.berkeley.edu/logo.cgi) (Crooks et al., 2004). CTR sequences are presented in Supplemental Figures 14–17.

Identification of RGAF Homologs

Most homologs were identified by protein BLAST at NCBI (http://blast.ncbi.nlm.nih.gov) using the RGAF sequence as a query. Accessions with a Max Score ≥800, a Query Cover ≥50%, an E-value ≤0.01, and an Identity ≥40% were classified as RGAF homologs. Homologs from the RGAP database (http://rice.plantbiology.msu.edu) and relevant articles were then identified manually using protein BLAST with the same thresholds (Supplemental Table 5).

Phylogenetic Trees

Phylogenetic trees were constructed using the MEGA 5.2.1 software (Tamura et al., 2011). The trees obtained by different methods, such as maximum likelihood, neighbor joining (NJ), and maximum parsimony, were similar, therefore, only the NJ trees with 1000 bootstrap replicates are shown. The full-length protein sequences of the RGAF homologs were used for Figure 7B. Full-length genomic sequences were used for Supplemental Figure 1B and 7A.

Allele Analysis in the Rice Germplasm Collection

A population of 520 rice cultivar accessions, including *indica subspecies (indica, Aus) and japonica rice (temperate japonica, tropical japonica),* from micro-core germplasm resources was planted in an experimental field at the Huazhong Agricultural University in the summer of 2019 (Xie et al., 2015). Due to a lack of sequence information for this locus in all cultivars, the allele analysis was based on the assumption that all the sequences were homologous to that of Nipponbare, including members and the number of *RGA* genes. *RGAf* allele types were identified by PCR using two pairs of gene-specific primers, Xa14-6F/Xa14-6R and Xa2-19F/Xa2-14R (Supplemental Table 8). The analysis was performed using sterilized water and the genomic DNA of Nipponbare, IRBB1, IRBB2, and IRBB14 as negative and positive controls.

Yeast Two-Hybrid Assays

Fragments containing different domains of *Xa14* or *Xa1* were amplified from the cDNAs of IRBB14 or IRBB1, respectively, using gene-specific primers (Supplemental Table 8). The products were then inserted into the pGBKT7 and pGADT7-Rec (Clontech) vectors by restriction endonuclease digestion and ligation. The paired constructs were co-transformed into the yeast strain AH109. Co-transformants were plated on synthetic medium without leucine, tryptophan, uracil, and histidine and incubated for 3 days at 28°C. The plasmids pGBKT7-53/pGADT7-RecT and pGBKT7-Lam/pGADT7-RecT were used as positive and negative controls, respectively. Each yeast two-hybrid assay was repeated at least twice with similar results, and only one replicate is presented.

Bimolecular Fluorescence Complementation Assay in Rice Protoplasts

Fragments encoding the BED domain of XA14 and XA1 were amplified using gene-specific primers and ligated into vectors pSPYCE(M) and pSPYNE173, respectively (Supplemental Table 8) (Waadt et al., 2008). Protoplasts were isolated from rice Oc suspension culture and transformed using a polyethylene glycol method as described by Shen et al. (2017). After incubation for 16–22 h at 30°C, the protoplasts were observed under a confocal microscope (FV1200; Olympus). Spectral settings for the detection of GFP fluorescence were excitation at 488 nm and detection at 500–525 nm.

Co-immunoprecipitation

Fragments containing the BED domain of XA14 or XA1 were amplified using gene-specific primers and ligated into the pU1031-9myc vector or the pU1301-3FLAG vector (Supplemental Table 8) (Yuan et al., 2016). The constructs were then introduced into the *A. tumefaciens* strain GV3101. *Agrobacterium*-mediated transformation was performed by infiltration into *Nicotiana benthamiana* leaves using needleless syringes. Proteins were extracted from *N. benthamiana* leaves, incubated with anti-FLAG beads (Sigma-Aldrich, St. Louis, USA), and washed as described previously (Ma et al., 2017). Western blot analyses were performed using anti-FLAG and anti-Myc antibodies (ABclonal, Wuhan, China). Co-immunoprecipitation analysis was repeated twice with similar results, and only one replicate is presented.

Statistical Analysis

Significant differences between control and treated samples were analyzed by pairwise *t*-test using Microsoft Office Excel (Microsoft, Redmond, WA, USA).

ACCESSION NUMBERS

Sequence data from this article can be found in the GenBank data libraries under the following accession numbers: MN794307 for *Xa1*, MN794308 for *Xa1-2*, MN794309 for *Xa14*, and MN794310 for *Xa31*(*t*).

SUPPLEMENTAL INFORMATION

Supplemental Information is available at *Plant Communications Online*.

FUNDING

This work was supported by grants from the National Natural Science Foundation of China (grant nos. 31821005, 31772145, and 31200912) and the China Scholarship Council (file no. 201908420054).

AUTHOR CONTRIBUTIONS

Conceptualization, H.Z. and S.W.; Methodology, B.Z., H.Z., and S.W.; Investigation, B.Z., F.L., H.Z., and S.W.; Writing – Original Draft, B.Z. and H.Z.; Writing – Review & Editing, H.Z. and S.W.; Funding Acquisition, H.Z. and S.W.; Resources, J.X. and X.L.; Supervision, M.Y. and Y.O.

ACKNOWLEDGMENTS

We thank Dr. Kaijun Zhao (Chinese Academy of Agricultural Sciences) and Prof. Gongyou Chen (Shanghai Jiao Tong University) for kindly providing rice seeds and the *Xoo* strain PB. The authors declare that they have no conflicts of interest.

Received: February 12, 2020
Revised: May 17, 2020
Accepted: June 16, 2020
Published: June 20, 2020

REFERENCES

Antony, G., Zhou, J., Huang, S., Li, T., Liu, B., White, F., and Yang, B. (2010). Rice xa13 recessive resistance to bacterial blight is defeated by induction of the disease susceptibility gene Os-11N3. Plant Cell **22**:3864–3876.

Aravind, L. (2000). The BED finger, a novel DNA-binding domain in chromatin-boundary-element-binding proteins and transposases. Trends Biochem. Sci. **25**:421–423.

Bailey, P.C., Schudoma, C., Jackson, W., Baggs, E., Dagdas, G., Haerty, W., Moscou, M., and Krasileva, K.V. (2018). Dominant integration locus drives continuous diversification of plant immune receptors with exogenous domain fusions. Genome Biol. **19**:23.

Bao, S., Tan, M., and Lin, X. (2010). Genetic mapping of a bacterial blight resistance gene Xa14 in rice. Acta Agronom. Sinica **36**:422–427.

Bernoux, M., Ve, T., Williams, S., Warren, C., Hatters, D., Valkov, E., Zhang, X., Ellis, J.G., Kobe, B., and Dodds, P.N. (2011). Structural and functional analysis of a plant resistance protein TIR domain reveals interfaces for self-association, signaling, and autoregulation. Cell Host Microbe **9**:200–211.

Boch, J., Scholze, H., Schornack, S., Landgraf, A., Hahn, S., Kay, S., Lahaye, T., Nickstadt, A., and Bonas, U. (2009). Breaking the code of DNA binding specificity of TAL-type III effectors. Science **326**:1509–1512.

Cesari, S., Thilliez, G., Ribot, C., Chalvon, V., Michel, C., Jauneau, A., Rivas, S., Alaux, L., Kanzaki, H., Okuyama, Y., et al. (2013). The rice resistance protein pair RGA4/RGA5 recognizes the *Magnaporthe oryzae* effectors AVR-Pia and AVR1-CO39 by direct binding. Plant Cell **25**:1463–1481.

Cheema, K.K., Grewal, N.K., Vikal, Y., Sharma, R., Lore, J.S., Das, A., Bhatia, D., Mahajan, R., Gupta, V., Bharaj, T.S., et al. (2008). A novel bacterial blight resistance gene from Oryza nivara mapped to 38 kb region on chromosome 4L and transferred to *Oryza sativa* L. Genet. Res. (Camb.) **90**:397–407.

Chen, H., Wang, S., and Zhang, Q. (2002). New gene for bacterial blight resistance in rice located on chromosome 12 identified from minghui 63, an elite restorer line. Phytopathology **92**:750–754.

Chen, J., Peng, P., Tian, J., He, Y., Zhang, L., Liu, Z., Yin, D., and Zhang, Z. (2015). Pike, a rice blast resistance allele consisting of two adjacent NBS-LRR genes, was identified as a novel allele at the Pik locus. Mol. Breed. **35**:1–15.

Chu, Z., Yuan, M., Yao, J., Ge, X., Yuan, B., Xu, C., Li, X., Fu, B., Li, Z., Bennetzen, J.L., et al. (2006). Promoter mutations of an essential gene for pollen development result in disease resistance in rice. Genes Dev. **20**:1250–1255.

Crooks, G.E., Hon, G., Chandonia, J.M., and Brenner, S.E. (2004). WebLogo: a sequence logo generator. Genome Res. **14**:1188–1190.

Deng, Y., Zhai, K., Xie, Z., Yang, D., Zhu, X., Liu, J., Wang, X., Qin, P., Yang, Y., Zhang, G., et al. (2017). Epigenetic regulation of antagonistic receptors confers rice blast resistance with yield balance. Science **355**:962–965.

Du, B., Zhang, W., Liu, B., Hu, J., Wei, Z., Shi, Z., He, R., Zhu, L., Chen, R., Han, B., et al. (2009). Identification and characterization of Bph14, a gene conferring resistance to brown planthopper in rice. Proc. Natl. Acad. Sci. U S A **106**:22163–22168.

Ellur, R.K., Khanna, A., S, G.K., Bhowmick, P.K., Vinod, K.K., Nagarajan, M., Mondal, K.K., Singh, N.K., Singh, K., Prabhu, K.V., et al. (2016). Marker-aided incorporation of Xa38, a novel bacterial blight resistance gene, in PB1121 and comparison of its resistance spectrum with xa13 + Xa21. Sci. Rep. **6**:29188.

Fukuoka, S., Yamamoto, S.-I., Mizobuchi, R., Yamanouchi, U., Ono, K., Kitazawa, N., Yasuda, N., Fujita, Y., Thi Thanh Nguyen, T., Koizumi, S., et al. (2014). Multiple functional polymorphisms in a single disease resistance gene in rice enhance durable resistance to blast. Sci. Rep. **4**:4550.

Gao, D.Y., Liu, A.M., Zhou, Y.H., Cheng, Y.J., Xiang, Y.H., Sun, L.H., and Zhai, W.X. (2005). Molecular mapping of a bacterial blight resistance gene *Xa-25* in rice. Yi Chuan Xue Bao **32**:183–188.

Gu, K., Tian, D., Qiu, C., and Yin, Z. (2009). Transcription activator-like type III effector AvrXa27 depends on OsTFIIAγ5 for the activation of Xa27 transcription in rice that triggers disease resistance to *Xanthomonas oryzae* pv. *oryzae*. Mol. Plant Pathol. **10**:829–835.

Gu, K., Yang, B., Tian, D., Wu, L., Wang, D., Sreekala, C., Yang, F., Chu, Z., Wang, G.L., White, F.F., et al. (2005). R gene expression induced by a type-III effector triggers disease resistance in rice. Nature **435**:1122–1125.

He, Q., Li, D., Zhu, Y., Tan, M., Zhang, D., and Lin, X. (2006). Fine mapping of Xa2, a bacterial blight resistance gene in rice. Mol. Breed. **17**:1–6.

Hu, K., Cao, J., Zhang, J., Xia, F., Ke, Y., Zhang, H., Xie, W., Liu, H., Cui, Y., Cao, Y., et al. (2017). Improvement of multiple agronomic traits by a disease resistance gene via cell wall reinforcement. Nat. Plants **3**:17009.

Hutin, M., Sabot, F., Ghesquiere, A., Koebnik, R., and Szurek, B. (2015). A knowledge-based molecular screen uncovers a broad-spectrum OsSWEET14 resistance allele to bacterial blight from wild rice. Plant J. **84**:694–703.

Jacob, F., Vernaldi, S., and Maekawa, T. (2013). Evolution and conservation of plant NLR functions. Front Immunol. **4**:297.

Ji, Z., Ji, C., Liu, B., Zou, L., Chen, G., and Yang, B. (2016). Interfering TAL effectors of Xanthomonas oryzae neutralize R-gene-mediated plant disease resistance. Nat. Commun. **7**:13435.

Kroj, T., Chanclud, E., Michel-Romiti, C., Grand, X., and Morel, J.B. (2016). Integration of decoy domains derived from protein targets of pathogen effectors into plant immune receptors is widespread. New Phytol. **210**:618–626.

Le Roux, C., Huet, G., Jauneau, A., Camborde, L., Tremousaygue, D., Kraut, A., Zhou, B., Levaillant, M., Adachi, H., Yoshioka, H., et al. (2015). A receptor pair with an integrated decoy converts pathogen disabling of transcription factors to immunity. Cell **161**:1074–1088.

Lin, Y., and Zhang, Q. (2005). Optimising the tissue culture conditions for high efficiency transformation of indica rice. Plant Cell Rep. **23**:540–547.

Liu, Q., Yuan, M., Zhou, Y., Li, X., Xiao, J., and Wang, S. (2011). A paralog of the MtN3/saliva family recessively confers race-specific resistance to *Xanthomonas oryzae* in rice. Plant Cell Environ. **34**:1958–1969.

Ma, H., Chen, J., Zhang, Z., Ma, L., Yang, Z., Zhang, Q., Li, X., Xiao, J., and Wang, S. (2017). MAPK kinase 10.2 promotes disease resistance

and drought tolerance by activating different MAPKs in rice. Plant J. **92**:557–570.

Ma, J., Lei, C., Xu, X., Hao, K., Wang, J., Cheng, Z., Ma, X., Zhou, K., Zhang, X., Guo, X., et al. (2015). Pi64, encoding a novel CC-NBS-LRR protein, confers resistance to leaf and neck blast in rice. Mol. Plant Microbe Interact. **28**:558–568.

Maekawa, T., Cheng, W., Spiridon, L.N., Toller, A., Lukasik, E., Saijo, Y., Liu, P., Shen, Q.H., Micluta, M.A., Somssich, I.E., et al. (2011). Coiled-coil domain-dependent homodimerization of intracellular barley immune receptors defines a minimal functional module for triggering cell death. Cell Host Microbe **9**:187–199.

Marchal, C., Zhang, J., Zhang, P., Fenwick, P., Steuernagel, B., Adamski, N.M., Boyd, L., McIntosh, R., Wulff, B.B.H., Berry, S., et al. (2018). BED-domain-containing immune receptors confer diverse resistance spectra to yellow rust. Nat. Plants **4**:662–668.

Mermigka, G., Amprazi, M., Mentzelopoulou, A., Amartolou, A., and Sarris, P.F. (2020). Plant and animal innate immunity complexes: fighting different enemies with similar weapons. Trends Plant Sci. **25**:80–91.

Meyers, B.C., Kaushik, S., and Nandety, R.S. (2005). Evolving disease resistance genes. Curr. Opin. Plant Biol. **8**:129–134.

Meyers, B.C., Kozik, A., Griego, A., Kuang, H., and Michelmore, R.W. (2003). Genome-wide analysis of NBS-LRR-encoding genes in *Arabidopsis*. Plant Cell **15**:809–834.

Ogawa, T., Morinaka, T., Fujii, K., and Kimura, T. (1978). Inheritance of resistance to rice varieties Kogyoku and Java 14. Annu. Phytopathol. Soc. Jpn. **49**:69–72.

Read, A.C., Moscou, M.J., Zimin, A.V., Pertea, G., Meyer, R.S., Purugganan, M.D., Leach, J.E., Triplett, L.R., Salzberg, S.L., and Bogdanove, A.J. (2020). Genome assembly and characterization of a complex zfBED-NLR gene-containing disease resistance locus in Carolina Gold Select rice with Nanopore sequencing. Plos Genet. **16**:e1008571.

Read, A.C., Rinaldi, F.C., Hutin, M., He, Y.Q., Triplett, L.R., and Bogdanove, A.J. (2016). Suppression of Xo1-mediated disease resistance in rice by a truncated, non-DNA-binding TAL effector of *Xanthomonas oryzae*. Front. Plant Sci. **7**:1516.

Romer, P., Recht, S., and Lahaye, T. (2009). A single plant resistance gene promoter engineered to recognize multiple TAL effectors from disparate pathogens. Proc. Natl. Acad. Sci. U S A **106**:20526–20531.

Shen, J., Liu, J., Xie, K., Xing, F., Xiong, F., Xiao, J., Li, X., and Xiong, L. (2017). Translational repression by a miniature inverted-repeat transposable element in the 3′ untranslated region. Nat. Commun. **8**:14651.

Song, W.Y., Wang, G.L., Chen, L.L., Kim, H.S., Pi, L.Y., Holsten, T., Gardner, J., Wang, B., Zhai, W.X., Zhu, L.H., et al. (1995). A receptor kinase-like protein encoded by the rice disease resistance gene, Xa21. Science **270**:1804–1806.

Sun, X., Cao, Y., Yang, Z., Xu, C., Li, X., Wang, S., and Zhang, Q. (2004). Xa26, a gene conferring resistance to *Xanthomonas oryzae* pv. *oryzae* in rice, encodes an LRR receptor kinase-like protein. Plant J. **37**:517–527.

Tamura, K., Peterson, D., Peterson, N., Stecher, G., Nei, M., and Kumar, S. (2011). MEGA5: molecular evolutionary genetics analysis using maximum likelihood, evolutionary distance, and maximum parsimony methods. Mol. Biol. Evol. **28**:2731–2739.

Tian, D., Wang, J., Zeng, X., Gu, K., Qiu, C., Yang, X., Zhou, Z., Goh, M., Luo, Y., Murata-Hori, M., et al. (2014). The rice TAL effector-dependent resistance protein XA10 triggers cell death and calcium depletion in the endoplasmic reticulum. Plant Cell **26**:497–515.

Triplett, L.R., Cohen, S.P., Heffelfinger, C., Schmidt, C.L., Huerta, A.I., Tekete, C., Verdier, V., Bogdanove, A.J., and Leach, J.E. (2016). A resistance locus in the American heirloom rice variety Carolina Gold Select is triggered by TAL effectors with diverse predicted targets and is effective against African strains of *Xanthomonas oryzae* pv. *oryzicola*. Plant J. **87**:472–483.

van Wersch, S., Tian, L., Hoy, R., and Li, X. (2020). Plant NLRs: the whistleblowers of plant immunity. Plant Commun. **1**:100016.

Waadt, R., Schmidt, L.K., Lohse, M., Hashimoto, K., Bock, R., and Kudla, J. (2008). Multicolor bimolecular fluorescence complementation reveals simultaneous formation of alternative CBL/CIPK complexes in planta. Plant J. **56**:505–516.

Wang, C., Zhang, X., Fan, Y., Gao, Y., Zhu, Q., Zheng, C., Qin, T., Li, Y., Che, J., Zhang, M., et al. (2015). XA23 is an executor R protein and confers broad-spectrum disease resistance in rice. Mol. Plant **8**:290–302.

Wang, C.T., Wen, G.S., Lin, X.H., Liu, X.Q., and Zhang, D.P. (2009). Identification and fine mapping of the new bacterial blight resistance gene, Xa31(t), in rice. Eur. J. Plant Pathol. **123**:235–240.

Wang, J., Hu, M., Qi, J., Han, Z., Wang, G., Qi, Y., Wang, H.W., Zhou, J.M., and Chai, J. (2019). Reconstitution and structure of a plant NLR resistosome conferring immunity. Science **364**:eaav5870.

Xie, W., Wang, G., Yuan, M., Yao, W., Lyu, K., Zhao, H., Yang, M., Li, P., Zhang, X., Yuan, J., et al. (2015). Breeding signatures of rice improvement revealed by a genomic variation map from a large germplasm collection. Proc. Natl. Acad. Sci. U S A **112**:E5411–E5419.

Xu, X., Lv, Q., Shang, J., Pang, Z., Zhou, Z., Wang, J., Jiang, G., Tao, Y., Xu, Q., Li, X., et al. (2014). Excavation of Pid3 orthologs with differential resistance spectra to *Magnaporthe oryzae* in rice resource. PLoS One **9**:e93275.

Yang, B., Sugio, A., and White, F.F. (2006). Os8N3 is a host disease-susceptibility gene for bacterial blight of rice. Proc. Natl. Acad. Sci. U S A **103**:10503–10508.

Yoshimura, S., Yamanouchi, U., Katayose, Y., Toki, S., Wang, Z.X., Kono, I., Kurata, N., Yano, M., Iwata, N., and Sasaki, T. (1998). Expression of Xa1, a bacterial blight-resistance gene in rice, is induced by bacterial inoculation. Proc. Natl. Acad. Sci. U S A **95**:1663–1668.

Yuan, M., Ke, Y., Huang, R., Ma, L., Yang, Z., Chu, Z., Xiao, J., Li, X., and Wang, S. (2016). A host basal transcription factor is a key component for infection of rice by TALE-carrying bacteria. Elife **5**:e19605.

Yuan, T., Li, X., Xiao, J., and Wang, S. (2011). Characterization of *Xanthomonas oryzae*-responsive *cis*-acting element in the promoter of rice race-specific susceptibility gene Xa13. Mol. Plant **4**:300–309.

Zhang, H., and Wang, S. (2013). Rice versus *Xanthomonas oryzae* pv. *oryzae*: a unique pathosystem. Curr. Opin. Plant Biol. **16**:188–195.

Zhang, H., and Wang, S. (2016). Progress in functional genomic studies of rice disease resistance. Chin. Bull. Life Sci. **28**:1189–1199.

Zhao, Y., Huang, J., Wang, Z., Jing, S., Wang, Y., Ouyang, Y., Cai, B., Xin, X.F., Liu, X., Zhang, C., et al. (2016). Allelic diversity in an NLR gene BPH9 enables rice to combat planthopper variation. Proc. Natl. Acad. Sci. U S A **113**:12850–12855.

Zhou, J., Peng, Z., Long, J., Sosso, D., Liu, B., Eom, J.S., Huang, S., Liu, S., Vera Cruz, C., Frommer, W.B., et al. (2015). Gene targeting by the TAL effector PthXo2 reveals cryptic resistance gene for bacterial blight of rice. Plant J. **82**:632–643.